The flow of micrometre-sized glass fibres in a replica of the human trachea

Frantisek Lizal[1,*], *Milan* Maly[1], *Matous* Cabalka[1], *Elena* Lizalova Sujanska[2], *Arpad* Farkas[1], *Pavel* Starha[1], *Kristyna* Kedajova[1], *Ondrej* Misik[1], *Ondrej* Pech[1], *Jan* Jedelsky[1], and *Miroslav* Jicha[1]

[1]Brno University of Technology, Faculty of Mechanical Engineering, Energy Institute, Technicka 2896/2 Brno, 616 60, the Czech Republic

[2]Department of Pulmonology and Allergology, Hospital Kromeriz, Havlickova 660/69, 767 01, Kromeriz, the Czech Republic

Abstract. Inhaled fibres can potentially cause inflammation of the lung tissue and interstitium which, after long-term exposure, may lead to lung cancer, malignant mesothelioma or pulmonary and pleural fibrosis. For risk reduction and correct setting of occupational hygiene regulations, it is important to be able to precisely calculate the fate of inhaled fibres depending on their physical characteristics and inhalation conditions. As there is a lack of experimental data on the orientation of fibres, a new test rig has been assembled for visualization and recording of flowing fibres in a replica of the human trachea. Fibres prepared from regular glass fibres produced commercially for blown thermal insulation have been processed, dispersed and introduced into the glass tube with dimensions of the trachea. Visualization was performed using a powerful LED light and a high-speed camera. Angles of the fibres have been evaluated for six different flowrates and the dependence of the angles on the flow Reynolds number was searched for. The angles of fibres agreed with expected values, i.e. only vertically and horizontally oriented fibres were recorded. However, the number of vertically and horizontally oriented fibres did not seem to be correlated with the flow Reynolds number.

1 Introduction

Inhaled fibres are recognized as pathogens that can potentially cause inflammation of the lung tissue and interstitium[a]. Pathogenicity of different fibres is not equal and there are many questions about the effects of man-made fibres and nanofibres. Generally speaking, the inhalation of fibres can lead to numerous adverse responses of the body, and the specific reaction depends on duration and intensity of the exposition, and character of fibres (their geometry and biopersistence[b]). The evidence reported e.g. in [1] shows that toxicity depends strongly on dimensions of fibres and less on the chemical composition of fibres.

Inhaled fibres tend to avoid the most efficient mechanism of lung clearance, i.e. slow upward movement of deposited particles together with mucus driven by the synchronised motion of cilia, which transports the fibres to the throat and the digestive system [2]. Some of the inhaled fibres penetrate and deposit beyond the ciliated airways, which, after the long-term exposure may lead to pulmonary and pleural fibrosis[c], i.e. asbestosis, pleural plaques[d], bronchogenic carcinoma[e] or malignant mesothelioma[f].

[a] An interstitial space within a tissue or organ. Here specifically meant the tissue between the pulmonary alveoli and the bloodstream.

[b] The ability to remain inside an organism, resistance to being forced out or digested.

[c] Pulmonary or pleural fibrosis is a diffuse accumulation of fibrous/scar tissue in the interstitium of the lung or in the pleura. Pulmonary fibrosis aggravates the diffusion of gases from the blood to the airspaces and restricts lung expansion. Pleural fibrosis may lead to pleural effusion - an accumulation of fluid in the pleural cavity.

[d] Pleural plaques are raised hard fibrous lesions (any damage or abnormal change in the tissue of an organism, usually caused by disease or trauma) that arise on the parietal pleura that are smooth and composed of a basketwork of pure collagen; they are almost acellular and do not seem to cause any adverse effects on the lungs.

[e] Bronchogenic carcinoma is a malignant cancer of the cells lining the bronchi or airways and is the same as the lung cancer that is common in smokers.

* Corresponding author: lizal@fme.vutbr.cz

Fibres can provoke an inflammatory reaction, but they can also directly start certain chemical processes. Acute or chronic inflammation is associated with oxidative stress and production and release of mediators[g]. [3] Fibres stimulate proliferation (rapid reproduction) of epithelial or mesothelial cells, and simultaneously during the inflammation, some chemical mediators attract fibroblasts[h], and it is deposited in the lung parenchyma in the area of the offending fibre. Fibres and mediators of inflammatory reaction can also lead to deletion of the gene coding or damage DNA (genotoxic effect) of these cells. These pathobiological processes can culminate in fibroplasia[i] and neoplasia[j].

The reason why the fibres manage to pass to the lower parts of the airways grounds in the fact that their aerodynamic diameter d_{ae} can be very low although their length may reach 30 or 50 μm. The d_{ae} is defined as a diameter of an equivalent sphere with the density of water (1000 kg/m^3) which has the same settling velocity as the particle in question. The equation that can be used for calculation of the d_{ae} (for cylindrical fibre) was derived by Griffiths and Vaughan [4]:

$$d_{ae} = d_f \sqrt{\frac{\rho_f \beta_a}{\rho_0 \chi}} \left(\frac{3}{2}\right)^{\frac{1}{3}}, \qquad (1)$$

where d_f is the physical diameter of the fibre, ρ_f is the fibre density, ρ_0 is the density of water (standard density), β_a is the aspect ratio, i.e. ratio of length to the diameter of the fibre, and χ is the dynamic shape factor, which has been defined as a ratio of the drag force on a non-spherical particle (fibre in our case) and the drag force of the volume equivalent sphere. Obviously, the fibre diameter influences the aerodynamic diameter more significantly than its length.

A troublesome situation is induced by the dynamic shape factor. Its value depends on the direction of the fibre motion with respect to the major axis of the fibre. Fuchs [5] has presented two equations, for parallel and perpendicular motion, respectively:

$$\chi_{\parallel} = \frac{\frac{4\left(\beta_a^2 - 1\right)}{3}}{\left\{\beta_a^{1/3} \frac{2\beta_a^2 - 1}{\sqrt{\beta_a^2 - 1}} \ln\left(\beta_a + \sqrt{\beta_a^2 - 1}\right) - \beta_a^{4/3}\right\}}, \qquad (2)$$

$$\chi_{\perp} = \frac{\frac{8\left(\beta_a^2 - 1\right)}{3}}{\left\{\beta_a^{1/3} \frac{2\beta_a^2 - 3}{\sqrt{\beta_a^2 - 1}} \ln\left(\beta_a + \sqrt{\beta_a^2 - 1}\right) + \beta_a^{4/3}\right\}}. \qquad (3)$$

In the cases, where the random orientation of fibres can be expected, following formula for the resulting dynamic shape factor can be used:

$$\frac{1}{\chi_{ran}} = \frac{1}{3}\left(\frac{1}{\chi_{\parallel}} - \frac{1}{\chi_{\perp}}\right). \qquad (4)$$

However, several papers (e.g. [6]) suggest that fibres tend to align with the flow in human lungs. Hence, parallel orientation should be preferential in human airways. On the other hand, Kulkarni [7] suggests, that the perpendicular orientation is preferential during gravitational settling and acceleration for particle Reynolds numbers $0.01 < Re_p < 100$ and that fibre motion is often treated as a combination of these two cases. In short, there is no general rule that would predict the number of fibres with parallel and perpendicular orientation as a simple function of flow and fibre characteristics. It should be noted, that this information is missing in models for prediction of deposition sites of inhaled fibres [8]. To improve the accuracy of such models, it is necessary to supplement them with precise data on the orientation of fibres.

The main aim of this work is to provide the missing experimental data on the preferential orientation of fibres in human airways. A new experimental rig has been assembled to allow visualization of the flow of micrometre-sized glass fibres originating from regular commercially produced glass wool which is applied routinely for blown thermal insulation of buildings. The test rig and the first results of the visualization performed on a replica of the human trachea are described in this contribution.

2 Materials and Methods

The glass wool Supafil® Loft (Knauf Insulation GmbH, Simbach am Inn, Germany) was used as a source of fibres. The wool has been disintegrated in a mechanical press in order to produce separate fibres. The diameter of

[f] Mesothelioma is an unusual tumour arising from the mesothelium lining the pleural space that is slow-growing and that does not metastasise and so is well-advanced before diagnosis leading subsequently to a very poor prognosis [2].

[g] Such as lysosomal enzymes, intermediates of arachidonic acid production, glutathione S-transferases, proteases, cytokines, growth factors, and reactive oxygen species (ROS - hydrogen peroxide, superoxide anion, hydroxyl radical) from pulmonary macrophages, neutrophils, and other inflammatory cells. ROS can be produced also in cell-free systems - as a direct chemical reaction between fibre surface and extracellular fluids

[h] A cell in connective tissue which produces collagen and other fibres.

[i] The formation of fibrous tissue, as normally occurs in the healing of wounds.

[j] An abnormal growth of tissue. Neoplasms may be benign (not cancer), or malignant (cancer).

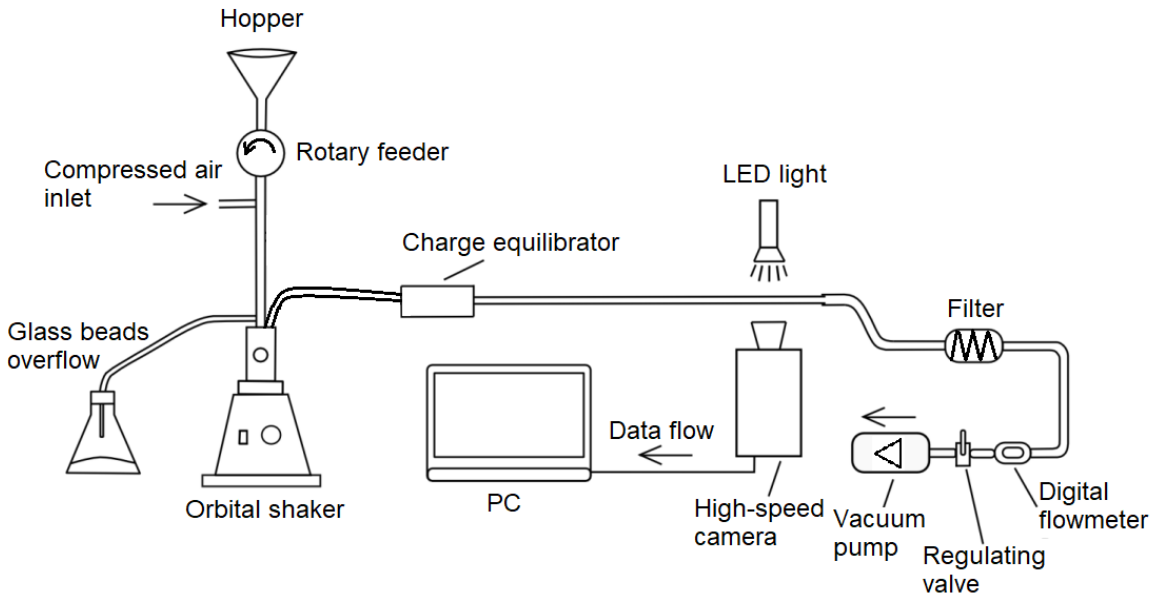

Fig. 1. A scheme of the experimental rig for visualization of flow of glass fibres in a replica of the human trachea.

fibres was 3.8±1.4 µm and the length was 34.1±19.0 µm. Then they were mixed with glass beads (Ballotini impact glass beads, Potters Industries Inc.) and sieved in order to deagglomerate the fibres and produce a homogenous mixture suitable for dispersing the fibres. The room air temperature during experiments was 20 to 21°C, hence the kinematic viscosity used for calculation of Reynolds number was 1.5×10^{-5} m^2/s, and density was 1.21 kg/m^3. The density of glass is approximately 2500 kg/m^3.

2.1 The experimental rig

The experimental rig (see Fig. 1) consisted of a reservoir of the mixture of glass beads and fibres (a hopper), a rotary feeder that provided a continuous supply of the mixture to a fluidized-bed-type disperser created from an orbital shaker Wisd NM-10 (Witeg Labortechnik GmbH, Wertheim, Germany) with an in-house extension. Fibres were charge equilibrated by ^{85}Kr neutralizer NEKR-10 (Eckert & Ziegler CESIO, Prague, the Czech Republic). The fibres than flowed through 1.5 m long glass tube to ensure the developed flow and were visualized by a high-speed camera. The flow was induced by a vacuum pump (Busch PA0008C, Busch Vakuum s.r.o., Brno, the Czech Republic) and measured by a digital flowmeter TSI 4040 (TSI, Shoreview, Minnesota, USA).

Table 1. An overview of the camera and light settings for all measured flowrates

Flow rate [l/min]	Image resolution (w×h) [px]	Frames per second [1/s]	Light pulse duration [ns]
2 l/min	1024×1024	5000	800
6 l/min	1024×1024	20000	800
12 l/min	1024×1024	20000	800
24 l/min	512×1024	35000	600
36 l/min	512×712	50000	500
48 l/min	512×512	60000	400

A high-speed camera Photron SA-Z was used to inspect the fibre flow inside a straight glass tube with an internal diameter of 15 mm. The long-range microscope lens 12X Zoom (NAVITAR, New York, USA) provided images with spatial a resolution of 1.5 µm per pixel. The flow was illuminated by a pulse LED light model HPLS-36DD18B (Lightspeed Technologies, USA). Since a wide range of the flow rates was used, the camera resolution and frame rate were changed in accordance with Table 1. Similarly, the light pulse duration varied in range from 400-800 ns.

Two cases were measured – at first a simple straight tube, then, the same tube was extended by a bifurcation (in the dimensions of the semi-realistic replica of the first bifurcation reported in [9]) and measured immediately upstream of the bifurcation. All measurements were performed in the axis of the tube, 20 mm upstream of the end of the straight tube.

The fibres appearing in a horizontal position in the images are parallel to the flow, the fibres recorded as vertical are perpendicular to the flow streamlines. Only fibres with either horizontal or vertical orientation were observed (in other words, there were no fibres with random orientation different from simply horizontal or vertical).

2.2 Statistical tests

The random variable X describing the quantity of horizontally oriented fibres is expected to have alternative (i.e. Bernoulli) distribution, or binomial distribution $Bi(1,p)$, respectively, where parameter p is the probability of horizontal fibre orientation. Hypothesis H_0: $p \geq 0.5$, therefore horizontally to vertically oriented ratio is higher than 1:1, is tested on significance level $\alpha = 0.05$. The following testing statistic is used.

$$T = \frac{\frac{X}{n} - p}{\sqrt{p(1-p)}}\sqrt{n}, \qquad (5)$$

T is the value of the testing statistic, X is the measured quantity of horizontally oriented fibres, p is parameter from the given hypothesis and n is total amount of measured fibres. For the given significance level α, a testing interval is $\overline{W_\alpha}$ = < -1.645, ∞) and if $T \in \overline{W_\alpha}$, the null hypothesis is not rejected.

3 Results and discussion

The following tables present data and results of the statistical analysis for measurements in a simple straight tube (Table 2) and in the tube upstream of a bifurcation (Table 3). The columns of the table contain flow rates, flow and particle Reynolds number, numbers of recorded horizontally and vertically oriented fibres, the total number of fibres, and the value of the testing statistics *T,* respectively.

Table 2. Results of the measurement and statistical analysis in the simple straight tube.

Flow rate	Re_f	Re_p	Horizontal	Vertical	Total	T
2 l/min	189	0.08	95	74	169	1.615
6 l/min	566	0.23	138	116	254	1.380
12 l/min	1132	0.45	226	194	420	1.561
24 l/min	2264	0.91	392	352	743	1.504
36 l/min	3395	1.36	146	116	262	1.853
48 l/min	4527	1.81	216	179	395	1.861

The column with values of testing statistics shows, that the null hypothesis (that there is more than 50% of horizontally oriented fibres) for any of the given flow rates in the simple straight tube can't be rejected on the significance level α.

Table 3. Results of the measurement and statistical analysis in the straight tube equipped with the bifurcation (the measurement was performed upstream of the bifurcation).

Flow rate	Re_f	Re_p	Horizontal	Vertical	Total	T
6 l/min	566	0.23	153	119	272	2.062
24 l/min	2264	0.91	182	142	324	2.222
36 l/min	3395	1.36	155	115	270	2.434

Consequently, the ratio of the number of horizontally and vertically oriented fibres (H/V ratio) was calculated for each flowrate and plotted against the flow Reynolds number (see Fig. 2). Obviously, there was no significant influence of the flow Reynolds number on the orientation of the fibres. The plot of H/V ratio as a function of particle Reynolds number gives almost identical results, as only the characteristic dimension differs (diameter of the tube switches to df).

It must be noted, that in the current setup only planar information can be acquired, i.e. seeing the fibres oriented along the flow or perpendicular to it means that the fibres do not rotate around the axis perpendicular to the visualized plane, however they may still rotate around the two in-plane axes (around an axis parallel to the flow when the fibre is seen perpendicular to the flow and around an axis perpendicular to the flow when seen aligned with the flow). This potential rotation cannot be detected.

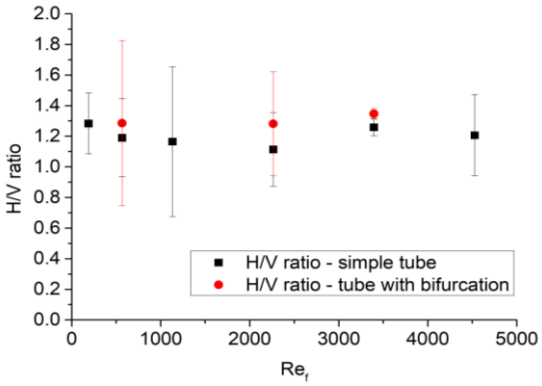

Figure 2. The ratio of horizontally and vertically oriented fibres as a function of the flow Reynolds number. The error bars show standard deviations.

4 Conclusions

The performed visualization proved that only fibres with orientation parallel or perpendicular to the streamlines appear in the axis of the simulated simplified trachea with the developed flow. Although the flow regimes ranged from laminar to turbulent, no significant dependence of the ratio of these two orientations on the Reynolds number was observed.

The null hypotheses that there is more than 50% of horizontally oriented fibres was not rejected in any of the measured cases, which suggests that the fibres tend to align with the flow which facilitates their penetration into the deep regions of the lungs. Further experiments will be performed to study the effects of harmonic breathing patterns on the orientation of the fibres.

Acknowledgement: This work was supported by the Czech Science Foundation under the grant GA18-25618S, and by the project FSI-S-17-4444.

References

1 K. Donaldson, F. A. Murphy, R. Duffin, and C. A. Poland, Particle and fibre toxicology 7 (2010).
2 K. Donaldson, C. A. Poland, F. A. Murphy, M. MacFarlane, T. Chernova, and A. Schinwald, Advanced Drug Delivery Reviews 65 (15), 2078 (2013).
3 O. Y. Osinubi, M. Gochfeld, and H. M. Kipen, Environ Health Perspect 108 Suppl 4, 665 (2000).
4 W. D. Griffiths and N. P. Vaughan, Journal of Aerosol Science 17 (1), 53 (1986).
5 N. A. Fuks, The mechanics of aerosols, Rev. and enl. ed. (Macmillan, New York,, 1964).
6 B. T. Mossman, M. Lippmann, T. W. Hesterberg, K. T. Kelsey, A. Barchowsky, and J. C. Bonner, J Toxicol Env Heal B 14 (1-4), 76 (2011).
7 P. Kulkarni, P. A. Baron, and K. Willeke, Aerosol measurement : principles, techniques, and applications, 3rd ed. (Wiley, Hoboken, N.J., 2011).
8 Á. Farkas, F. Lizal, J. Elcner, J. Jedelsky, and M. Jicha, Journal of Aerosol Science 136, 1 (2019).
9 F. Lizal, J. Elcner, P. K. Hopke, J. Jedelsky, and M. Jicha, Proceedings of the Institution of Mechanical Engineers Part H-Journal of Engineering in Medicine 226 (H3), 197 (2012).